

## Seismic interactions between suspended ceilings and nonstructural partition walls

Wen-Chun Huang\*, Ghyslaine McClure<sup>a</sup> and Nahidah Hussainzada<sup>b</sup>

*Department of Civil Engineering and Applied Mechanics, McGill University,  
817 Sherbrooke Street West, Montreal, Quebec H3A 0C3, Canada*

*(Received August 1, 2013, Revised February 13, 2014, Accepted February 14, 2014)*

**Abstract.** This study aims at observing the coupling behaviours between suspended ceilings and partition walls in terms of their global seismic performance using full-scale shake table tests. The suspended ceilings with planar dimensions of 6.0 m × 3.6 m were tested with two types of panels: acoustic lay-in and metal clip-on panels. They were further categorized as seismic-braced, seismic-unbraced, and non-seismic installations. Also, two configurations of 2.7 m high partition wall specimens, with C-shape and I-shape in the plane layouts, were tested. In total, seven ceiling-partition-coupling (CPC) specimens were tested utilizing a unidirectional seismic simulator. The test results indicate that the damage patterns of the tested CPC systems included failure of the ceiling grids, shearing-off of the wall top railing, and, most destructively, numerous partial detachments and falling of the ceiling panels. The loss of panels was mostly concentrated near the center of the tested partition wall. The testing results also confirmed that the failure mode of the non-seismic CPC systems was brittle: The whole system would collapse suddenly all at once when the magnitude of the inputs hit the capacity threshold, rather than displaying progressive damage. Overall, the seismic capacity of the unbraced and braced CPC systems could be up to 1.23 g and 2.67 g, respectively; these accelerations were both achieved at the base of the partition wall. Nonetheless, for practical applications, it is noteworthy that the three-dimensional nature of seismic excitations and the size effect of the ceiling area are parameters that exacerbate the CPC's seismic response so that their actual capacity may be dramatically decreased, leading to important losses even in moderate seismic events.

**Keywords:** suspended ceiling systems; partition walls; seismic performance; operational and functional components; shake table tests; nonstructural components; OFC

### 1. Introduction

The seismic hazards of nonstructural building components (also known as operational and functional components, OFCs) have often been underestimated in design. OFCs are seismically vulnerable and they can be damaged even when the seismic excitations are of low to medium intensities (Jaimes *et al.* 2013 and Filiatrault *et al.* 2011). This was demonstrated once again in a recent moderate earthquake of magnitude 6.1 in Ren-AI, Taiwan on March 27, 2013: very few structural failures have been reported but there was severe damage to vulnerable OFCs such as

---

\*Corresponding author, Postdoctoral Researcher, E-mail: [wen-chun.huang@mcgill.ca](mailto:wen-chun.huang@mcgill.ca)

<sup>a</sup> Professor, E-mail: [ghyslaine.mcclure@mcgill.ca](mailto:ghyslaine.mcclure@mcgill.ca)

<sup>b</sup> Graduated Master, E-mail: [nahidah.hussainzada@mail.mcgill.ca](mailto:nahidah.hussainzada@mail.mcgill.ca)

several suspension ceiling collapses in office buildings (<http://tw.news.yahoo.com/lightbox/南投6-1強震-slideshow/好像921-30秒4級震動-台中驚嚇破表-photo-004407109.html>). This is yet another of many similar past events that should increase the awareness of building design professionals to the importance of the good seismic performance of OFCs and the needs for prevention and mitigation of the seismic hazards to OFCs in existing buildings to ensure public safety.

Among the many types of architectural OFCs, this study is concerned with the suspension ceiling systems and partition walls that are very common to most important public buildings, including hospitals, schools, and offices. Previous architectural engineering research has addressed seismic mitigation measures for suspended ceilings and partition walls, but separately, as two independent OFCs (Gilani *et al.* 2010, Huang *et al.* 2010, Lee *et al.* 2007, Filiatrault *et al.* 2004 and Yao 2000). For instance, Ryu *et al.* (2012) conducted shake table experiments on 15 suspension ceiling configurations with an area of 100 m<sup>2</sup> and found that the ceilings without lateral supports are vulnerable when their area and loading are large. Retamales *et al.* (2013) performed racking tests on 3 steel-framed gypsum partition walls of partial height and with top seismic braces attached to the slab above. The observed damages included buckling of the seismic braces and failure of the connections between the braces and the top tracks. The same study also concluded that the seismic behaviours of the partition walls vary significantly even if the same materials, construction details and installation personnel have been provided. This conclusion corresponds to that of Huang *et al.* (2010): The performance of the partition walls can be improved if the installation and the joint details are of good workmanship, otherwise they are seismically vulnerable. As a result, several national codes, standards, and official documents have recommended that such OFCs should be braced to structural floors to improve their seismic security (ASCE 2010, ASTM 2011, CSA 2011, Foo *et al.* 2007 and Fierro *et al.* 1994). In particular, ASTM E580M-11b (ASTM International 2011) stipulates that the top of partition walls, when being tied to the suspension ceiling systems, shall be laterally braced to the building structure. The US Gypsum Association (<http://www.gypsum.org/>) also recommends that partial height partition walls shall be seismically braced to the structural slab above in both



Fig. 1 Typical office space with partitions jointed to suspended acoustical ceilings

longitudinal and transverse directions, using diagonal steel stud members identical to the members of wall framing, as the specimen installation details applied in the study by Retamales *et al.* (2013). In construction practice, nevertheless, suspension ceiling systems are usually installed in large open areas, and then the installation of partition walls follows, dividing the large areas into several smaller spaces, as shown in Fig. 1 for example in an office building environment. Also, most of these light-weight partition walls are designed to be dismountable and easily re-organized, so a rigid anchorage of the partitions to the building structure will conflict with this feature. Therefore, rather than bracing the partition to structural floors, installers usually joint the top of partition walls to suspended ceiling grids. Since this type of partition walls have not been extended to the structural floor above, rather than being inter-story drift sensitive as conventional drywall partitions (Retamales *et al.* 2013, Lee *et al.* 2007, McMullin and Merrick 2007), they are considered as acceleration sensitive (Huang *et al.* 2010, Filiatrault *et al.* 2004). To better understand the implications of this installation practice on seismic risk, this study aims at observing the interactions between suspended ceilings and partition walls to investigate their global seismic behaviour and performances using full-scale shake table tests.

In this experimental program, two groups of suspension ceiling systems with planar dimensions of 6.0 m  $\times$  3.6 m were tested with two types of panels: classical acoustical lay-in ceilings (ALC) and metal clip-on panels (MCP). Each group was subcategorized into seismic-braced, seismic-unbraced, and non-seismic installations. Also, two configurations of partition wall specimens were tested, with C-shape and I-shape in the planar layout and 2.7 m in height. In total, seven ceiling-partition-coupling (CPC) specimens were tested utilizing a uni-directional seismic simulator in the Structural Laboratory at École Polytechnique de Montréal, Canada. The goal of the study was not to conduct the seismic qualification/certification (Retamales *et al.* 2011 and ICC-ES 2010) of the CPC systems, but rather to study their overall behaviour under seismic excitations of different intensities. The seismic inputs in this study were generated from numerical SAP models, based on the top floor responses of two existing Montreal buildings subjected to several earthquake base motions matching the seismic hazards in Montreal and Vancouver as stipulated in the National Building Code of Canada, as well as a near-fault motion record of the 1999 ChiChi Earthquake (Magnitude 7.3 on September 21, 1999) in Taiwan (Shin and Teng 2001, Loh and Tsay 2001). Test results include damage patterns, seismic responses as well as dynamic characteristics. Besides, the loss percentage of panels and the seismic capacity of each tested CPC system were also investigated. It is noteworthy that these capacities were estimated according to the specific ceiling area tested with one-dimensional inputs applied in the principal directions. For practical applications, the effects of three-dimensional excitations, size of the surface area, and the loading conditions of the ceiling are important parameters, which were verified in the study of Ryu *et al.* (2013). These parameters are known to exacerbate the CPC's seismic response so the actual capacity of similar specimens in their normal environment may be dramatically decreased, potentially leading to important losses even in moderate seismic events.

## 2. Experimental study

### 2.1 General testing layout

The tests were conducted utilizing a 3.4 m  $\times$  3.4 m seismic simulator. In order to support the CPC specimens, an extension testing platform of 4.3 m  $\times$  6.7 m was built and connected to the

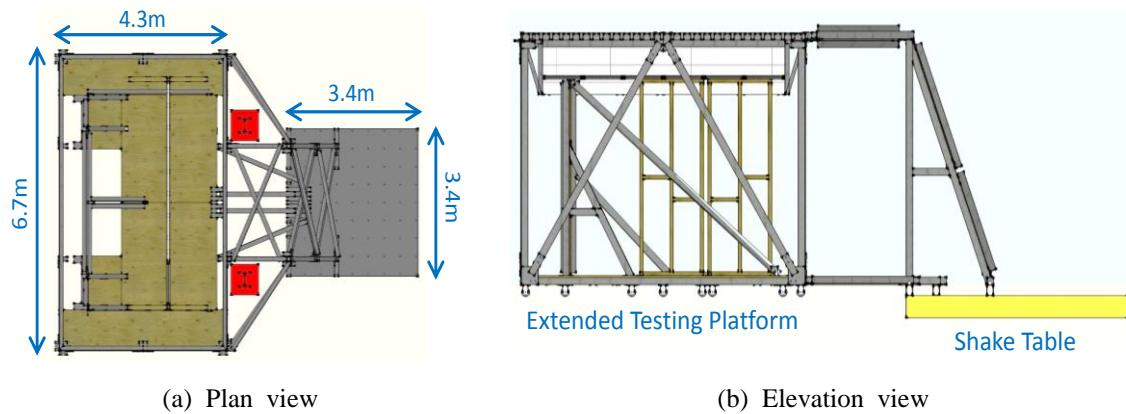


Fig. 2 The shake table and testing platform

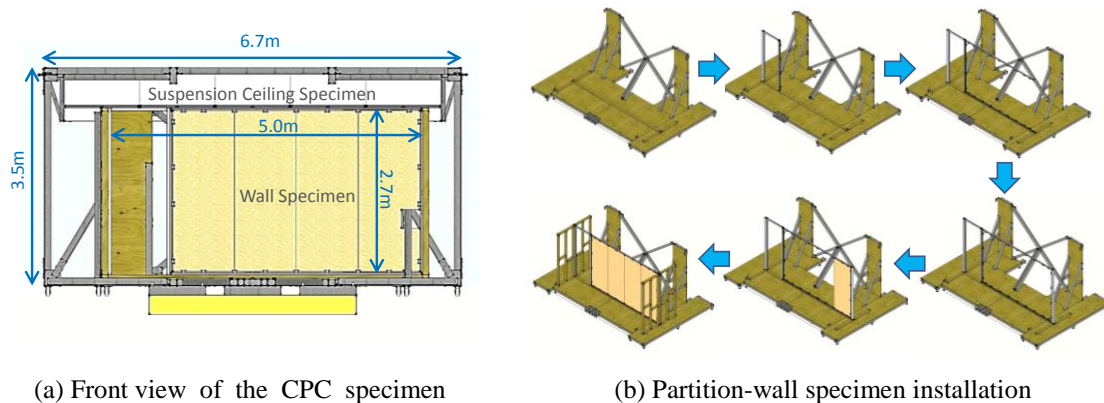


Fig. 3 The testing Ceiling Partition Coupling (CPC) specimens

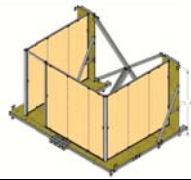
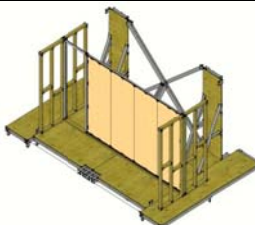
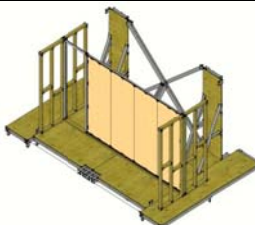
shake table, as shown in Figs. 2(a) and (b). In Fig. 2(b), the extended testing platform is attached at both the top and bottom to the A-frames directly mounted on the shake table. The acceleration inputs of the shake table can therefore be transmitted to the testing platform during the tests. Since the testing set-up configuration does not allow studying inter-story drift effects, only acceleration effects are considered and discussed in this study. The dimension of the I-shape wall specimen is 5.0 m in width and 2.7 m in height, connected to a planar 6.0 m  $\times$  3.6 m suspension ceiling specimen installed above it, as shown in Fig. 3(a). Fig. (b) illustrates the installation stages for the I-shape partition wall specimen, including: layout on the floor, setup of the top and bottom railings, and installation of the wall panels.

## 2.2 Tested specimens

In total, seven ceiling-partition-coupling (CPC) specimens were tested, as listed in Table 1. The C-shape partition wall specimen was to simulate a typical 3.0m $\times$ 4.0m $\times$ 3.0m office space, while the I-shape specimens were tested to represent the longer partition walls of corridors in common practice.

practice.

Table 1 The tested CPC specimens

Specimen No.	Ceiling installation	Wall mass (kg)	Ceiling panel types	Wall configuration
1-1	Seismic-Unbraced	500	Metal Clip-on Panels (MCP)	
2-1	Seismic-Braced	200	Acoustical Lay-in Ceilings (ALC)	
2-2	Seismic-Unbraced	200		
2-3	Non-Seismic	200		
3-1	Seismic-Braced	200	Metal Clip-on Panels (MCP)	
3-2	Seismic-Unbraced	200		
3-3	Non-Seismic	200		

Notes

- Seismic: Installation of the suspension ceiling specimens in accordance with ASTM E580.
- Non-seismic: Installation of the suspension ceiling specimens following the common practice in North America, i.e. T-grid suspended to floor structure above using metallic hanger wires with no specific requirements applied.
- Material of the wall panels: Medium-density fibreboard ( $1000 \text{ kg/m}^3$ , thickness: 1.5 in. (38 mm))

In Table 1, the non-seismic installation of suspension ceiling refers to the general practice using hanger metal wires without any seismic consideration. For the seismic installation, the suspension ceiling systems shall be installed in accordance with the ASTM E580 requirements for the design categories D, E and F, and some important requirements are summarized as follows:

- Only heavy-duty main tees as defined in ASTM C635 shall be used.
- The support ledge of the wall moulding shall be of at least two-inch (50 mm) long and a gap of three quarters of an inch (19 mm) shall be held.
- The main tees shall be attached to the wall on two adjacent sides.
- The main runners shall be suspended at a maximum spacing of 48 inches (1220 mm).
- At the perimeter of the ceiling, the cross and the main runners shall be hung at a maximum distance of 8 inches (203 mm) from the walls.
- Stabilizer bars shall be used within 24 inches (610 mm) of the walls at the two floating edges to prevent the spread of the cross-tees.
- Lateral bracing systems are required for all ceiling areas greater than  $1000 \text{ ft}^2$  ( $93 \text{ m}^2$ ).

A schematic comparison among the seismic-braced, seismic-unbraced, and non-seismic installations of the suspension ceiling systems is shown in Fig. 4. The seismic system is installed with moulding attachments, stabilizer bars and with a larger amount of hanger wires than the non-seismic ceilings: these measures can improve the seismic resistance of ceiling systems to withstand strong earthquakes. More details about the characteristics and seismic behaviour of suspension ceiling systems tested without the presence of wall partitions can be found in Huang *et al.* (2013).

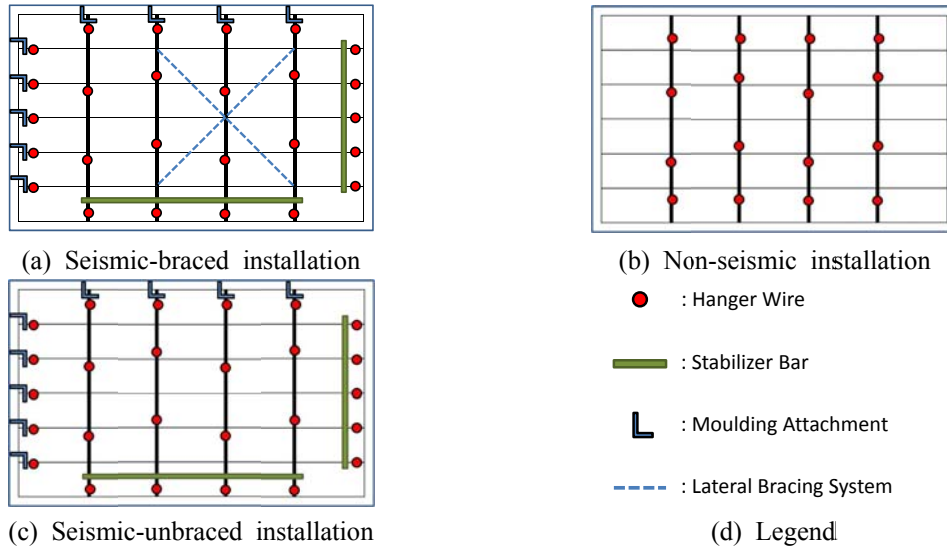


Fig. 4 Schematic representation of the seismic-braced, seismic unbraced, and non-seismic installations of suspension ceiling systems

2.3 Instrumentation

Schematic illustrations of the instrumentation used in the tests are shown in Fig. 5. For the suspension ceiling (Fig. 5(a)), four accelerometers and four displacement meters were used to measure the motions of the main grid lines, SC1, SC2, SC3, and SC4, aligned in the main shaking direction (East-West). Fig. 5(b) shows that three accelerometers and six displacement meters were installed to measure the response motions of the partition walls; the motions of the extension platform were also monitored. The arrows in the figure indicate the measuring direction of the sensors.

2.4 Shake table input motions

As mentioned in the introduction, the seismic inputs were generated from numerical SAP models, based on the top floor responses of two existing Montreal buildings subjected to several

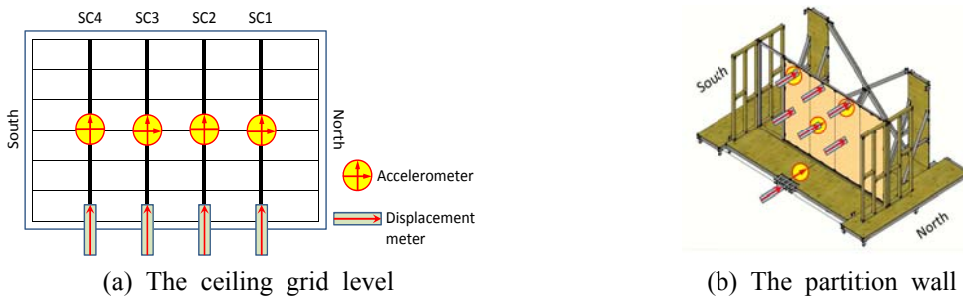


Fig. 5 Instrumentation of the CPC specimens

Table 2 The seismic horizontal inputs to the shake table

Input sequence	Seismic input designation	Target peak acceleration (g)	Peak acceleration achieved on the testing platform floor (g)
1	A_M10%_E70_300	0.11	0.14
2	B_M10%_E70_200	0.26	0.25
3	A_V10%_W72_100	0.35	0.26
4	B_V10%_W60_50	0.55	0.76
5	A_ChiChi_T76_50	0.46	0.52
6	B_ChiChi_T76_50	0.40	0.45
7	A_M2%_E70_100	0.53	0.49
8	A_V2%_W72_70	0.67	0.50
9	B_M2%_E70_70	0.74	0.86
10	B_V2%_W65_50	1.04	1.23
11	A_ChiChi_T76_15	1.38	2.67

## Notes

- A indicates top floor response of Building A
- B indicates top floor response of Building B
- M: Montreal, V: Vancouver, %: Percentage probability of exceedance in 50 years
- For example, A\_M10%\_E70\_300 indicates: Top floor acceleration response of Building A under Eastern Canada earthquake input with magnitude  $M_w$  7.0 at 300 km from the epicenter.

earthquake motions that match the seismic hazards in Montreal and Vancouver as stipulated in the National Building Code of Canada (Atkinson and Beresnev 1998), as well as a near-fault motion record of the 1999 ChiChi Earthquake in Taiwan. Their main characteristics are as listed in Table 2. Building A and Building B are two existing reinforced concrete shear wall (RCSW) buildings in Montreal, Canada with 27 and 14 stories in heights, respectively.

In Table 2, the achieved acceleration peaks of the testing platform illustrate that with the same exceedance probability in 50 years, the western Canadian (Vancouver) seismic events have higher intensity than in eastern Canada (Montreal). Moreover, the top floor acceleration responses of Building B are larger than those of Building A under the same excitation level, because the taller Building A has a longer fundamental period (2.17 s vs. 0.71 s) and is therefore less sensitive to the frequency content of the seismic inputs selected. In Fig. 6, the calculated horizontal acceleration amplification factors of the floors from the SAP2000 numerical models of both buildings are plotted. The reliability of the two simulation models have been verified by comparing and calibrating their lowest natural frequencies to the values extracted from ambient vibration tests on the real buildings in Montreal, Canada (Gilles and McClure 2008). Figs. 6(a) and (b) show that Building A experiences higher mode vibrations, while Building B has more violent response (more amplification) when subjected to the same seismic events. Therefore, when the CPC specimens were subjected to the Building A events, resonances were more likely to occur due to their richer frequency content within the range of the building frequencies.

Fig. 7 compares the FFT spectra of the targeted and achieved accelerations. It is seen that the dominant frequency contents of both building events are below 10 Hz, and in this range the achieved accelerations on the floor of the testing platform agreed with the target acceleration inputs except for the achieved building B events had slight overshooting at 9 Hz.

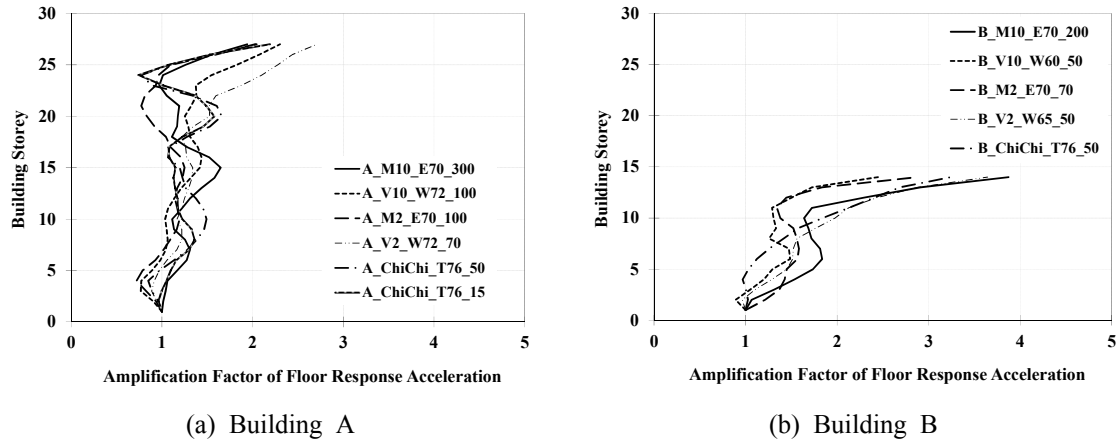


Fig. 6 Variation of the calculated maximum acceleration amplification factors along building height for selected input motions

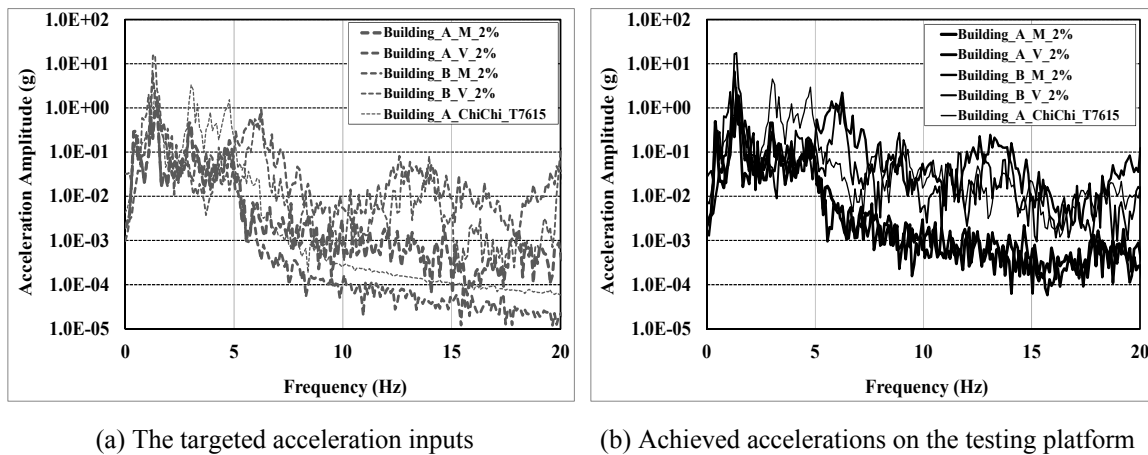


Fig. 7 FFT spectra of the targeted and achieved acceleration inputs on the floor of the testing platform

### 3. Testing results

#### 3.1 Specimen installation procedures

Fig. 8 illustrates the sequence of the installation procedure and details of partition wall specimens. As a first step, the corner posts and railings of the wall were attached to the ceiling grids by angle brackets and screws, as shown in Figs. 8(a) and (b). The completed perimeter framework of the walls is shown in Fig. 8(c). Several plastic brackets - the main components holding the wall panels, were then installed inside the top and bottom railings, as shown in Fig. 8(d). These plastic brackets are attached to the floor and ceiling grid runners, with two bolts along their longitudinal axis to adjust the level of the wall panels. After the wall panels are put in place, they are fastened by screws at their upper L-shape part. In Fig. 8(e), the first panel of the wall was being placed, and Fig. 8(f) shows the completed I-shape partition wall installation.



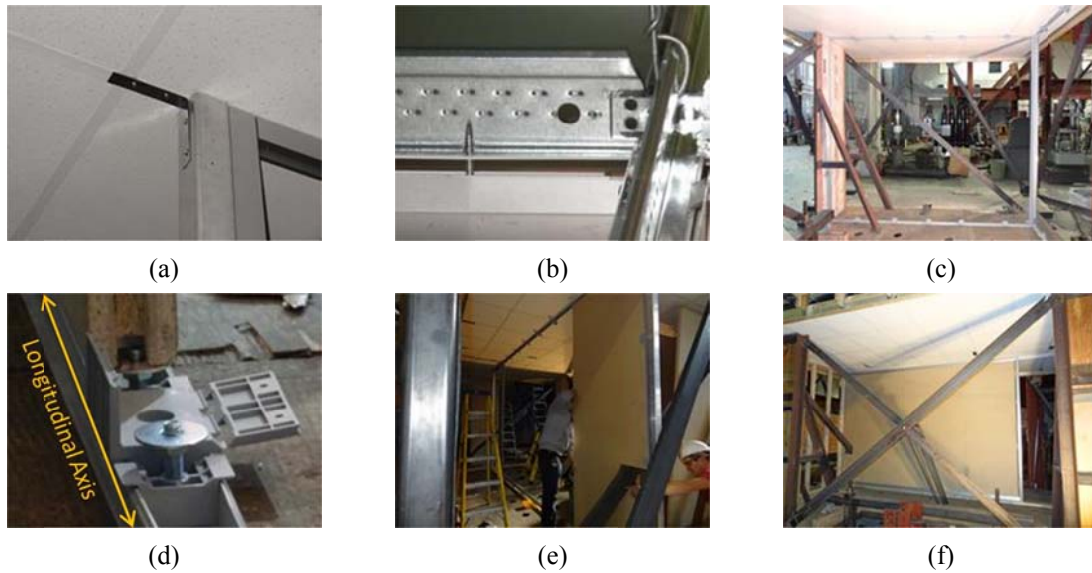


Fig. 8 The installation procedure of the partition wall specimen

### 3.2 Seismic-unbraced MCP with C-shape wall

Fig. 9(a) shows the installed specimen before testing. In this test series, no obvious failure was observed until the 2.67 g A\_ChiChi\_T7615 input was applied (input sequence 11 in Table 2), after which partial dislocation of one panel and failure at the top of the front wall occurred, as shown in Fig. 9(b). The brackets, as marked in Fig. 9(c), were sheared-off from the wall top railing. Furthermore, as shown in Fig. 9(d), the top hinge of the door (left open during the test) was damaged.

No damage was found in the suspension ceiling system after the test, indicating that the connection between the suspension ceiling system and the front wall was not strong enough to transmit the seismic force completely from the partition wall to the ceiling grid; this in turn created the potential hazard of toppling of the front wall panels. Therefore, in the following test series, the I-shape walls perpendicular to the direction of seismic inputs were studied with different details



(a) Set-up before testing (b) Panel dislocation and wall damage (c) Shearing-off of the top wall brackets (d) Damage to the door top hinge

Fig. 9 Testing results of the seismic-unbraced MCP with C-shape wall specimen

to investigate their interaction with the suspension ceiling systems. For the I-shape wall specimen, the wall length was 5 m inclusive of a 1m-wide opening at the corner (space for door), and the number of plastic brackets installed at the wall top was increased from 4 to 9, in comparison to the C-shape wall specimen.

### 3.3 Acoustic lay-in ceilings (ALC) with I-shape walls

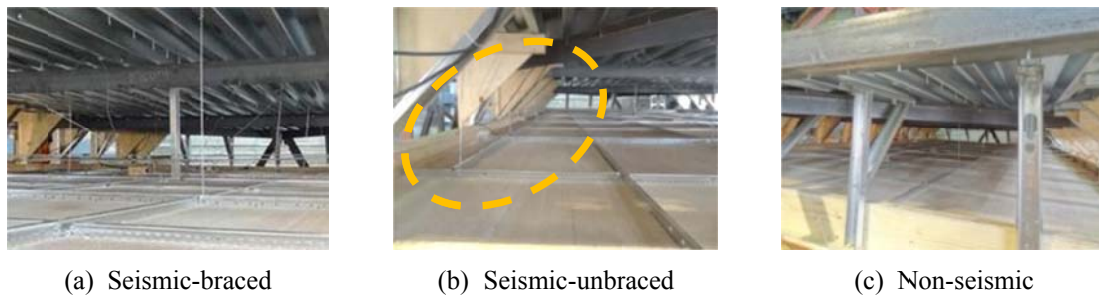


Fig. 10 Three different installations of the suspension ceiling systems

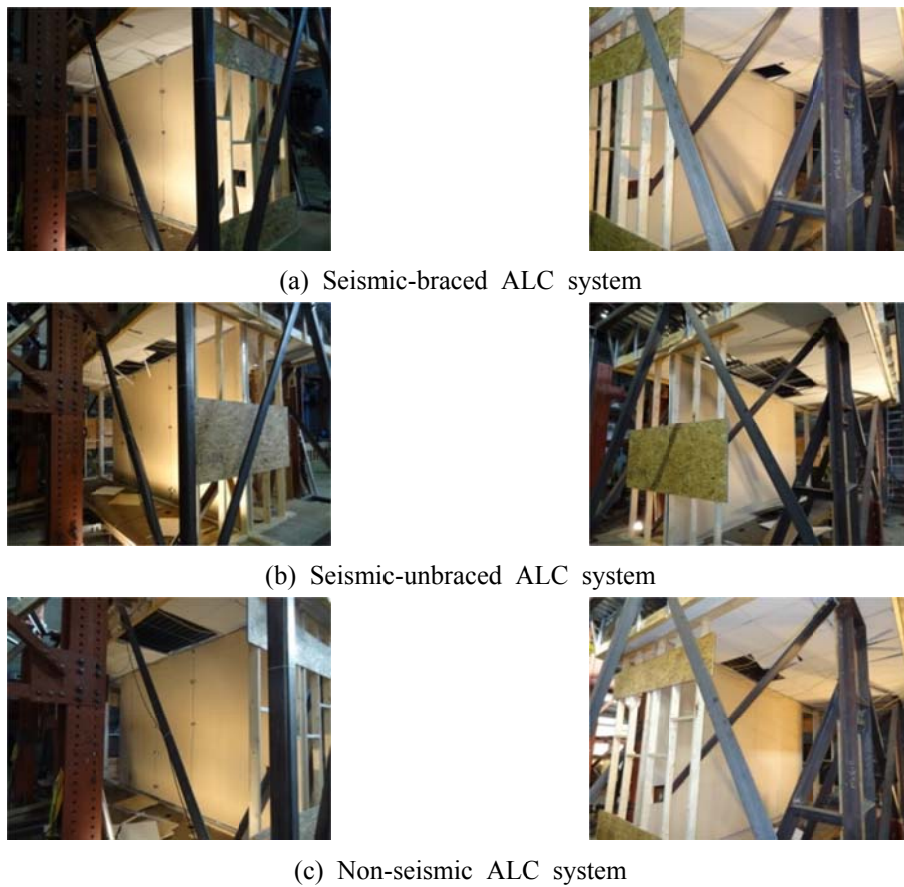


Fig. 11 The specimens of the Acoustic Lay-in Ceiling group after testing

In the second group of specimens, the acoustic lay-in ceilings of different installing conditions with I-shape walls were tested. The three different installations of the suspension ceiling systems are compared in the plenum views of Fig. 10. The ceiling bracing system is shown in Fig. 10(a). Fig. 10(b) shows that the unbraced seismic installation includes edging hanger wires and stabilizer bars on the runners, as enclosed by the dashed oval line.

In this test series, some minor damages to local joints were found after A\_V2 and B\_V2 inputs to the seismic-unbraced specimen. The damaged incurred to this testing group after completion of the eleven seismic inputs is shown in Fig. 11. For the seismic-braced specimen, only one panel fell after the A\_ChiChi\_T7615 input as shown in Fig. 11(a), showing that the bracing system significantly enhanced the seismic resistance of the whole. For the seismic-unbraced specimen, several panels fell with most of them located near the center of gravity of the wall, as shown in Fig. 11(b). Besides, shear-off failure of the grids occurred on the top of the wall and a few of the 4' (1219 mm) cross-tees buckled due to the lateral compression induced by the 2' (610mm) cross-tees. Failure of the non-seismic specimen, as shown in Fig. 11(c), was localized in the interval above the center of the partition wall (between ceiling grids SC1 and SC2) because this system did not act as an integral structure, so the ceiling grids could move separately: it is a floating system without lateral restraint, so the ceiling grid displacements were relatively large. Severe damage to both the wall top railings and ceiling grids above them also occurred.

### 3.4 Metal clip-on panels (MCP) with I-shape walls

The metal panels with the clip-on mechanism (see Fig. 12(a)) were tested in the final testing series. When installed, the panel surface is lower than the bottom of the ceiling grids and their butt-edge detail makes the ceiling grids hidden behind the panels, as shown in Figs. 12(b) and (c). This butt-edge detail could provide some stiffness and restrain the horizontal displacements of the ceiling system.

The testing results of the MCP group specimens after completion of the eleven testing inputs are shown in Fig. 13. For the seismic-braced specimen, in Fig. 13(a), only three panels fell and no damage to the ceiling grid was visible.

For the seismic-unbraced specimen in Fig. 13(b), more panels had fallen and dislocated as well as a few grid joints were damaged, with most of them against the wall top. Fig. 13(c) shows the severe damage of the non-seismic specimen. The failure mode of the non-seismic CPC system was brittle: the whole system collapsed suddenly all at once when the magnitude of the inputs hit the capacity threshold, without signs of progressive damage. A wide range of failure mechanisms,

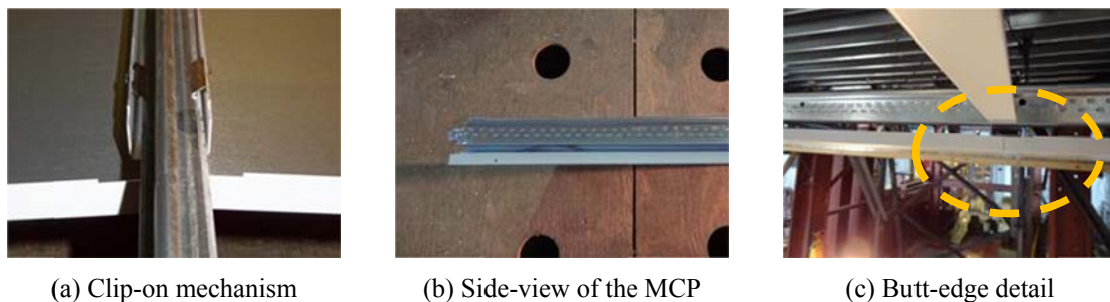


Fig. 12 Installation details of the metal clip-on panels

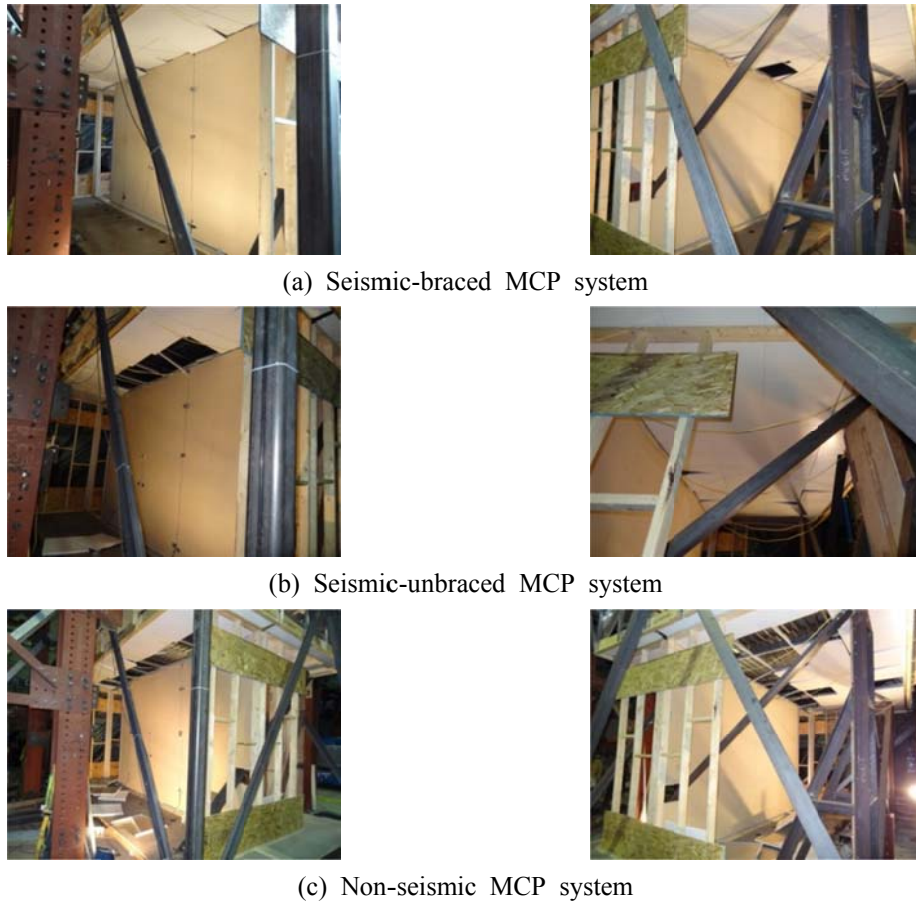


Fig. 13 The specimens of the Metal Clip-on Panel group after test

including panel loss and grid damage, occurred even though the MCPs had the clip-on and butt-edge characteristics. These results emphasize the important role of the ceiling bracing in improving the overall performance of the system and reducing the risk of brittle ceiling failures.

They also indicate that reinforcing only the panels (with edging hanger supports and stabilizing bars) is not an efficient seismic mitigation option. The entire suspension ceiling system should be seismically retrofitted with multidirectional bracings to significantly improve the seismic performance of the integrated wall partition/suspended ceiling systems.

## 4. Discussion

### 4.1 Natural frequencies of the tested specimens

At the beginning of every test series, a white noise (WN) signal with duration of 300 s and amplitude of 0.1 g was inputted to the testing platform to investigate the dynamic properties of the specimens. The natural frequencies (NF) of the seismic-braced and non-seismic specimens were

then extracted using Discrete Fourier Transform analysis of the acceleration records. From the results shown in Fig. 14, the NFs of the ceiling systems (ceiling main grid SC2 is selected as representative of the whole system) were ranging between 12.0 Hz -14.0 Hz and the seismic installation only increase the values slightly. For ALC specimens, it is clear that the behaviour of

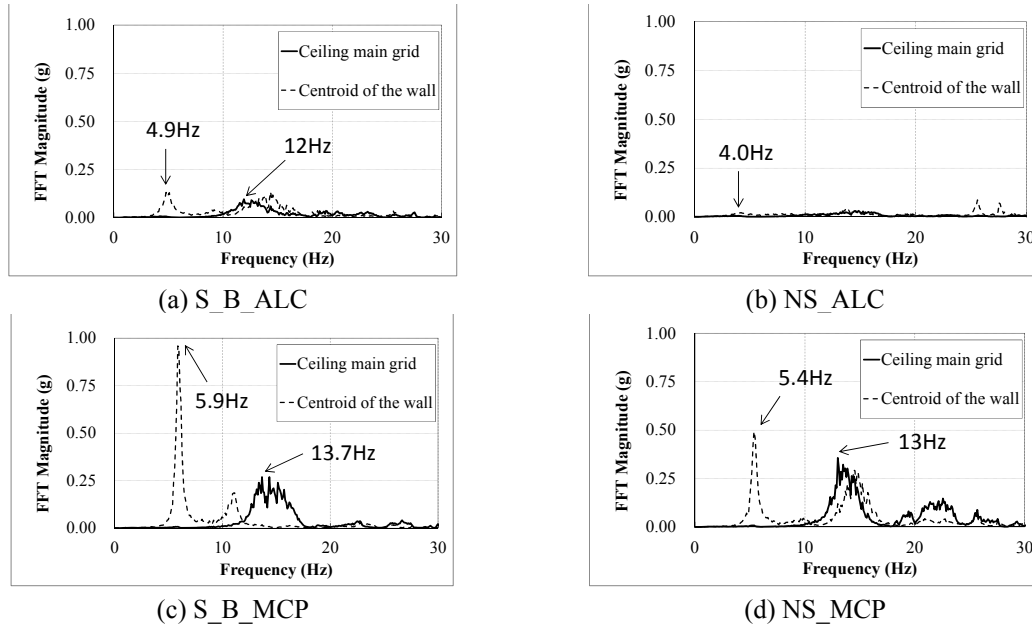


Fig. 14 FFT spectra of the ceiling main grid SC2 and the partition wall of the tested specimens

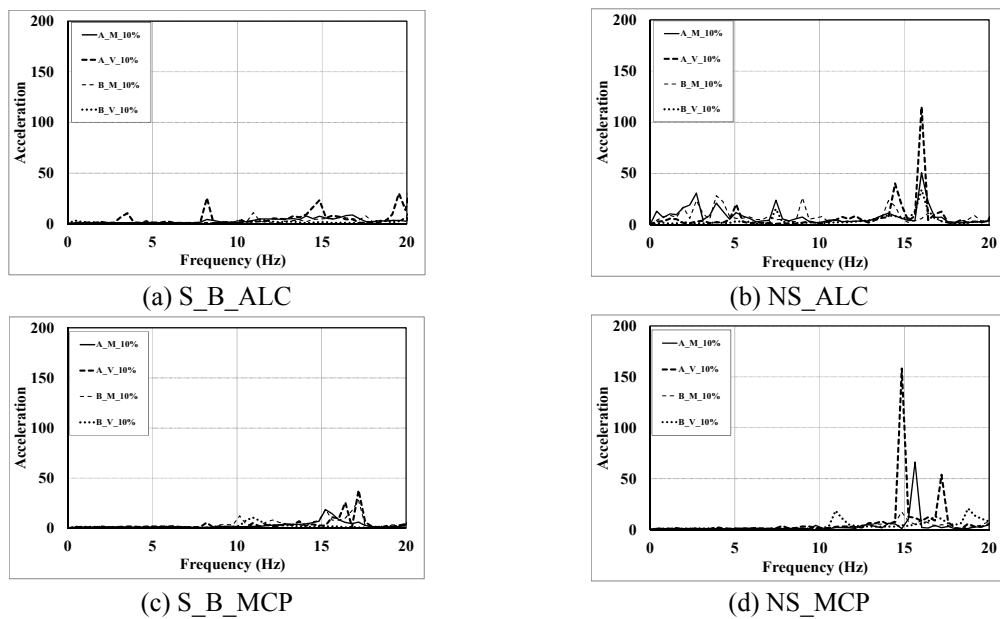


Fig. 15 Comparison of the FRF of the ceiling main grids with respect to testing platform floor under low to moderate excitations



the non-seismic specimens was dominated by frictional damping because the response amplitude of the system is low and their NFs are blurred with a wide bandwidth in the FFT spectra. For Metal MCP specimens, the WN input was too weak to generate inertial forces that could overcome the inherent frictional damping of the clip-on mechanism, even for the non-seismic specimens. Nevertheless, the NFs of the wall specimens were sensitive to different methods of ceiling installation and panel types: For instance, the NF of the non-seismic ALC I-shape wall specimen was not sharp but approximately 4.0 Hz, and for the seismic-braced MCP, it increased to 5.9 Hz.

In contrast with the low intensity WN input, the frequency response functions (FRF) of the ceiling grids with respect to the floor of the testing platform are shown in Fig. 15, for inputs with low to moderate intensities. Fig 15(b) shows that for the non-linear ALC specimens, the system's inherent frictional forces had been overcome during testing and the dominant frequencies of the ceiling grids had then been lowered to below 5 Hz. For the MCP specimens, their dominant frequencies had not changed significantly even if the clip-on mechanism has provided stiffer resistance. However, greater excitations also caused higher acceleration responses of the non-seismic installations for MCP specimens.

#### 4.2 Seismic response of the tested CPC specimens

In this section, the seismic response of the ceiling grids is discussed in terms of their accelerations and displacements for the SC2 main runner line (see Fig. 5), deemed representative of the whole.

In Fig. 16, the Building B events were more violent than those of Building A, causing larger acceleration responses. However, at the input level of 0.5 g, Building A events induced larger accelerations. This phenomenon is explained by the richer frequency content of Building A floor response and therefore the increased likelihood of resonances with the specimens. The acceleration response of the different ceiling installations is similar below 4.0 g. Larger accelerations (above 8.0 g) were measured for the non-seismic specimens due to the effect of pounding impact (shock) of the swaying ceiling on the perimeter moulding.

Fig. 17 shows the displacement response of the seismic-braced and non-seismic ALC specimens. It confirms that the displacements of the seismic system were effectively limited to less than 10mm, especially at SC2 (with less than 5 mm) in the vicinity of the bracing system. For the non-seismic systems, the measured displacements were larger, up to 15mm.

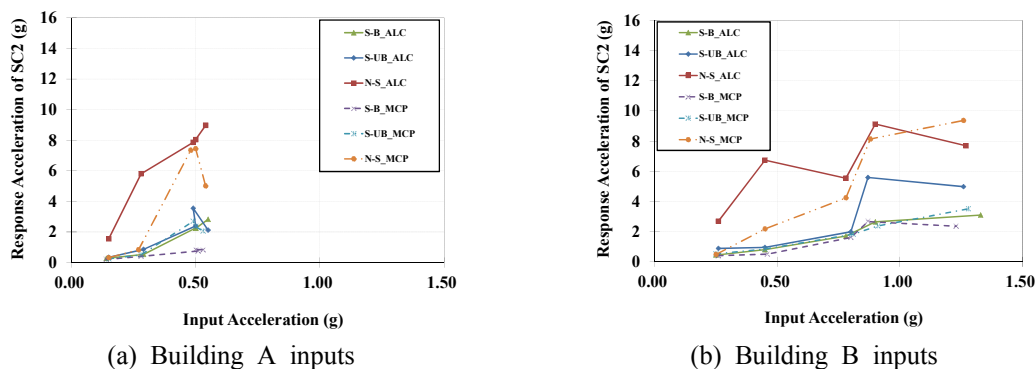


Fig. 16 Acceleration response of ceiling gridline SC2 of the tested specimens

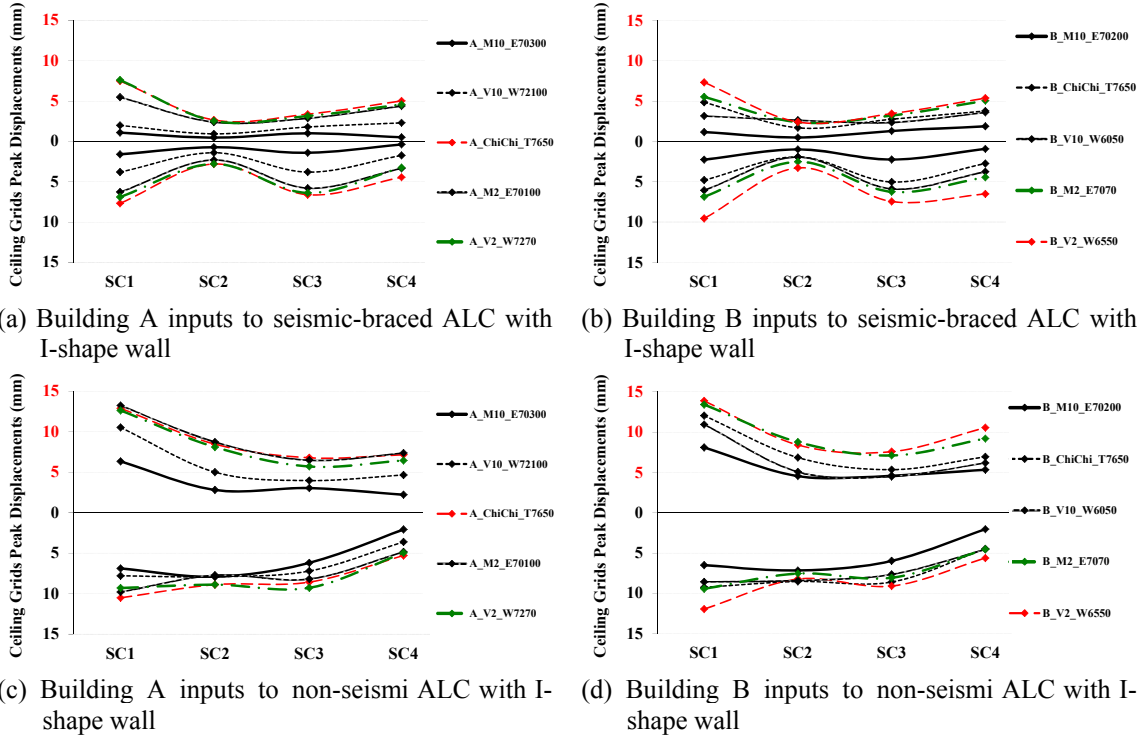


Fig. 17 Displacement response of the tested ceiling grids

Fig. 18 also compares the SC2 grid line displacement response of various tested specimens under different input acceleration levels achieved on the floor platform. It is seen that the Building B events generated higher input accelerations and therefore caused larger displacements than Building A events. However, the displacement response to Building A inputs was dramatically increased above 0.5 g, which is explained by the richer frequency content of the inputs, as previously discussed. Also, when the input levels increased to above 0.5 g, the inherent frictional resistances of the specimen were mostly overcome by inertia forces and the displacement response increased accordingly. Overall, when all the tested systems are compared at all acceleration input levels, the seismic-braced MCP specimen had the lowest displacement response (i.e., it was the stiffest) and the non-seismic ALC specimen had the largest (i.e., the specimen was the most flexible), as expected.

The seismic response of the tested I-shape wall specimens is shown in Fig. 19. In most cases, both the acceleration and displacement responses were increased with the input level, and, similarly to the ceiling grids, the wall specimens of the non-seismic systems responded more violently than the walls in other systems. The maximum values reached for Building B inputs were above 4.0 g and 50 mm. Besides, there is one special case shown in Fig. 19(b) where the acceleration responses of the seismic-braced MCP specimen were significantly higher than that of other specimens under the effects of Building B inputs. This is explained by a tuning (resonance) between the NF of the seismic-braced MCP wall (5.9 Hz as shown in Fig. 14(c)), and the high energy content of the Building B inputs near 6.0 Hz (input spectra were derived but not shown due to space limitations). This also confirms that this partition wall specimen belongs to the

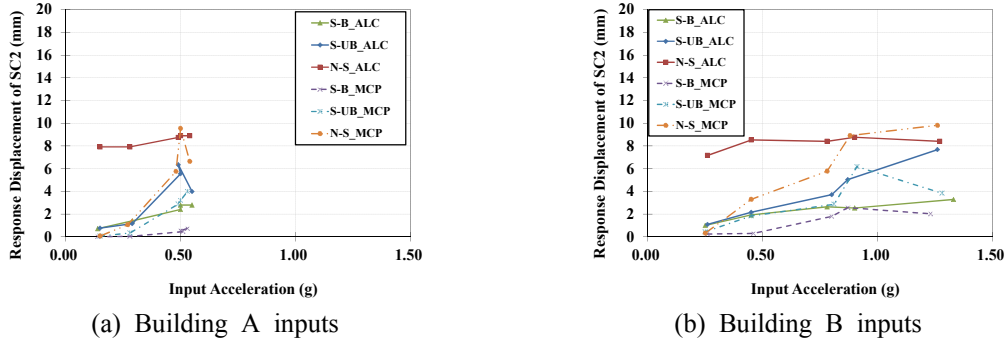


Fig. 18 Displacement response of ceiling gridline SC2 of the tested specimens

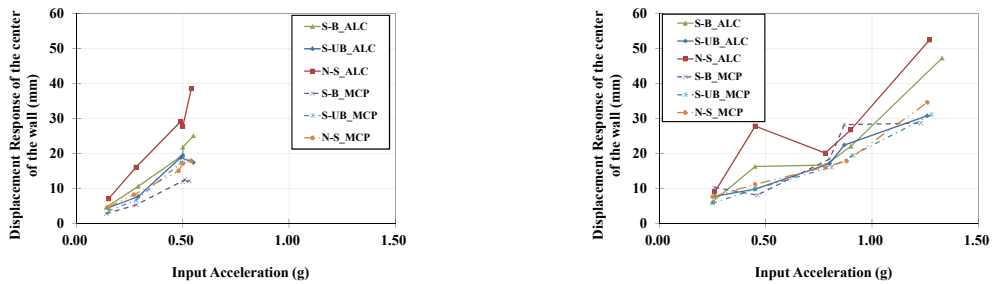
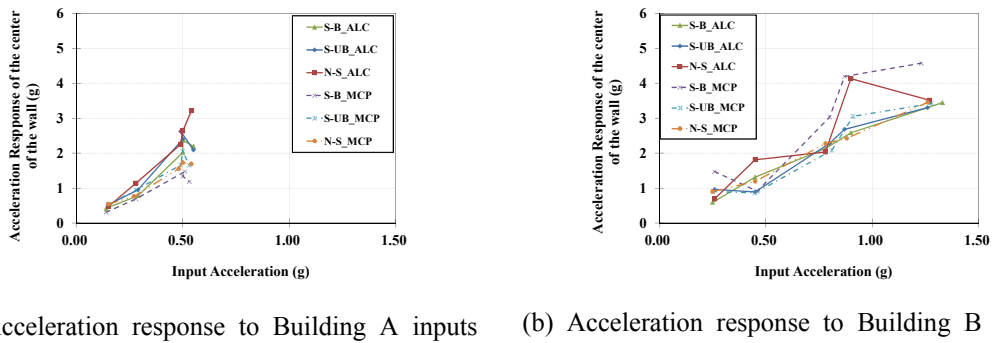


Fig. 19 The maximum dynamic response measured for I-shape wall specimens

acceleration-sensitive OFCs when considering its out-of-plane response and the frequency components of the floor excitations can cause significant dynamic amplifications of the response if local resonances (tuning) occur.

#### 4.3 Damage patterns and distribution of the tested CPC specimens

The damage patterns observed in the tested specimens are summarized in Fig. 20, including damages of ceiling grid and joints (Figs. 20(a) to (c)), distortion of wall top railing (Fig. 20(d)), as well as panel failure (Figs. 20(e) and (f)).



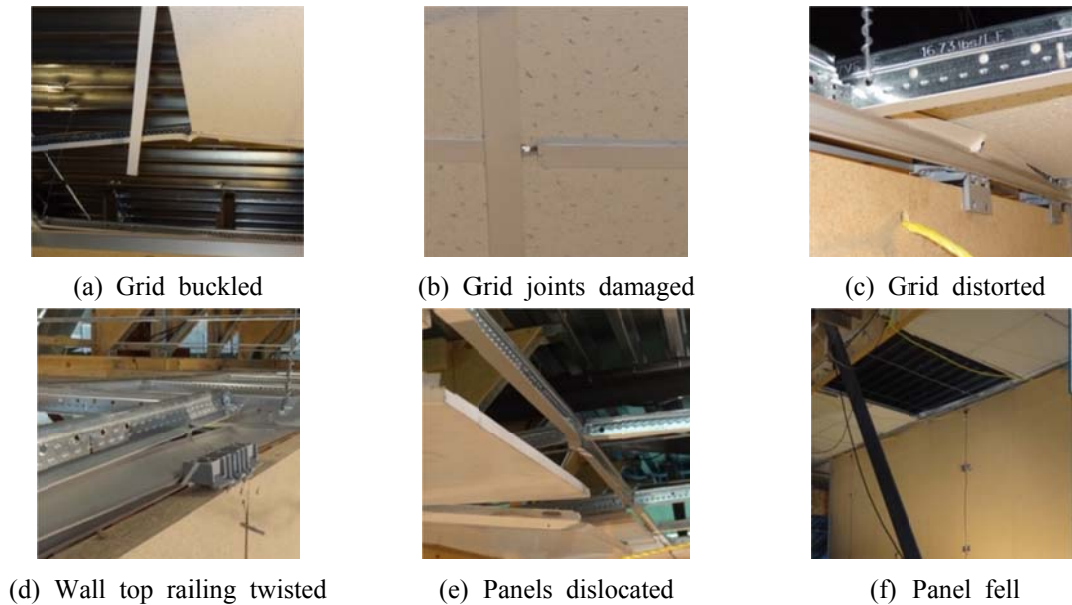


Fig. 20 Ceiling damage patterns of the tested CPC specimens

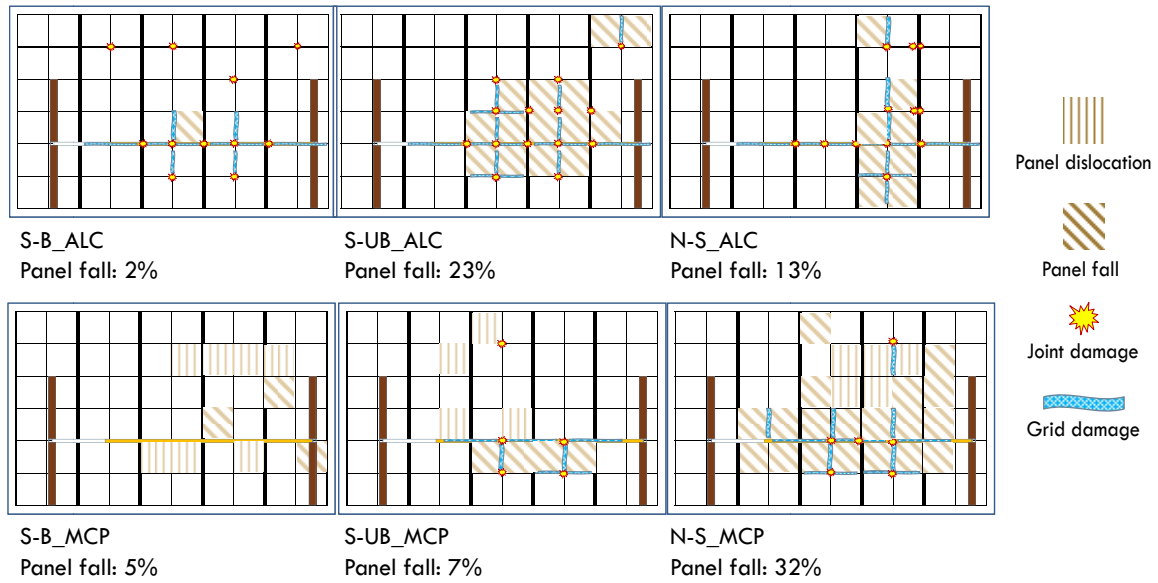


Fig. 21 Summary of ceiling damage distribution of the tested CPC specimens

Overall, more grid and joint damages were observed on the ALC specimens than on the MCP, for the MCP provides additional horizontal stiffness to the suspension grid systems. Twisted top railing was most severe in the non-seismic ALC specimens as they experienced high acceleration and displacement responses. As for panel failures, both the ALC and MCP groups had more than 20% panel falling when the ceiling systems were installed without lateral bracing.

A summary of the damage distribution of the tested CPC specimens is shown in Fig. 21. The braced seismic ceiling system can limit the percentage of ceiling-panel falling to less than 5%. The unbraced seismic ceiling system could not be as effective due to its dynamic interaction with the partition wall, irrespective of the use of lay-in (ALC) or clip-on (MCP) ceilings. The MCP ceiling system can concentrate and limit grid joint damage in the vicinity of the wall partition while the ALC ceiling system shows more distributed damage propagation away from the wall partition. Furthermore, the failure of non-seismic ALC was localized within the interval between grids SC1 and SC2, indicating that the non-seismic ALC specimen did not respond as an integral system. Of course, such observations are limited to the tested specimens and cannot be generalized to all similar systems because the actual response is strongly dependent on the geometric characteristics of the tested layouts (surface area, connection details, workmanship) and the input excitations (intensity and direction). Interactive and propagating damage patterns are expected to be much more complex in real situations.

## 5. Conclusions

In this study, seven ceiling-partition-coupling (CPC) specimens were constructed and tested on a shake table platform. Several Canadian design earthquakes and some records from the 1999 ChiChi Earthquake in Taiwan, including one near-fault event, were selected to generate the inputs to the testing platform. In the experimental program, the uni-directional input excitation was perpendicular to the longitudinal direction of the suspension ceiling systems and the I-shape wall specimens. The salient findings of the study are as follows:

- For seismic suspension ceiling systems:
  1. Panel loss could be controlled to less than 5% provided the ceiling bracing system with compression strut was installed. This ceiling bracing can help improve the overall performance of the ceiling/wall partition system and reduce damage of the ceiling system.
  2. The metal clip-on panel (MCP) group performed better than the acoustical lay-in ceiling system (ALC) in terms of the reduced seismic response, as the butt-edge detail improved the robustness of the system.
  3. The seismic-unbraced system could not withstand the strong excitation of A\_ChiChi\_T7615, as ceiling bracing is needed to carry such a large near-fault earthquake force.
  
- For non-seismic suspension ceiling systems:
  1. The ceiling damage of the non-seismic ALC group was concentrated within a certain interval between two main ceiling grid lines next to the wall partition, as there was no possible seismic load path to the whole system.
  2. The seismic response of the non-seismic specimens was higher than that of the seismic systems due to the lack of lateral restraint, causing severe damage to both the ceiling grids and the wall top railings.
  3. Although the non-seismic MCP specimen was with the clip-on devices, it also experienced high percentage of panel loss when subjected to extremely strong excitation (near-fault ChiChi building floor response).

- In this study, the seismic capacities of the CPC specimens could be up to 1.23 g. For the seismic-braced systems, it could reach 2.67 g. However, these accelerations were unidirectional and achieved at the platform floor level. For practical situations, three-dimensional inputs and area size effects should be considered which would likely reduce the CPC capacities
- Testing inputs of Building B seismic events are more violent than Building A, causing greater seismic responses of the CPC specimens. However, localized resonance could occur with the Building A inputs due to their rich frequency content.

## Acknowledgments

The extension testing platform was built with technical support provided by John Bartczak at McGill University. The seismic tests were conducted at the Structures Laboratory of École Polytechnique de Montréal with the assistance of testing engineer Martin Leclerc. The partition wall specimens were provided and installed by Rampart Partitions Inc. under approval from CEO and owner Robert Elhen, and the ceiling materials were provided by Armstrong/Simplex Ceilings of Montreal with the support of plant manager Michel Desjardins. All of these contributions are greatly acknowledged. This research was funded by Strategic Research Project Grant STPGP 396464 from the Natural Sciences and Engineering Research Council of Canada (NSERC), and by Fonds Québécois pour la Recherche Nature et Technologie (FQRNT), regroupement stratégique CEISCE, Centre d'études interuniversitaire sur les structures sous charges extrêmes.

## References

- ASCE (2010), *Minimum design loads for buildings and other structures*, ASCE/SEI 7-10, ASCE, Reston, VA, USA.
- ASTM (2011), *Standard practice for application of ceiling suspension systems for acoustical tile and lay-in panels in areas subject to earthquake ground motions*, ASTM E580M-11b, ASTM International, West Conshohocken, PA, USA.
- Atkinson, G.M. and Beresnev, I.A. (1998), "Compatible ground-motion time histories for new national seismic hazard maps", *Can. J. Civil Eng.*, **25**(2), 305-318.
- Canadian Standards Association (2011), *Standard for seismic risk reduction of operational and functional components for buildings*, CSA-S832-06(R2011), Rexdale, ON, Canada.
- Fierro, E.A., Perry, C.L. and Freeman, S.A. (1994), *Reducing the risks of nonstructural earthquake damage - A practical guide*, The Federal Emergency Management Agency (FEMA), Washington, DC, USA.
- Filiatrault, A., French, S., Holmes, W., Hutchinson, T., Maragakis, E. and Reitherman, R. (2011), "Research on the seismic performance of nonstructural components", *Proceedings of the 2011 Architectural Engineering Conference*, Oakland, California, USA, March.
- Filiatrault, A., Kuan, S. and Tremblay, R. (2004), "Shake table testing of bookcase - partition wall systems", *Can. J. Civil Eng.*, **31**(4), 664-676.
- Foo, S., Ventura, C. and McClure, G. (2007), "An overview of a new canadian standard on the seismic risk reduction of operational and functional components of buildings", *Proceedings of the 9th Canadian Conference on Earthquake Engineering*, Ottawa, ON, Canada, June.
- Gilani, A.S.J., Reinhorn, A.M., Glasgow, B., Lavan, O. and Miyamoto, H.K. (2010), "Earthquake simulator testing and seismic evaluation of suspended ceilings", *J. Archit. Eng. - ASCE*, **16**(2), 63-73.
- Gilles, D. and McClure, G. (2008), "Development of a period database for buildings in Montreal using ambient vibrations", *Proceedings of the 14th World Conference on Earthquake Engineering (14WCEE)*,

- Beijing, China, October.
- [Http://www.gypsum.org/](http://www.gypsum.org/)
- [Http://tw.news.yahoo.com/lightbox/南投-6-1-強震-slideshow/好像-921-30-秒-4-級震動-台中-驚嚇破表-photo-004407109.html](http://tw.news.yahoo.com/lightbox/南投-6-1-強震-slideshow/好像-921-30-秒-4-級震動-台中-驚嚇破表-photo-004407109.html)
- Huang, W.C., Hussainzada, N. and McClure, G. (2013), "Experimental study on the seismic behaviour of suspended ceilings", *Proceedings of the Canadian Society for Civil Engineering (CSCE) 3rd Specialty Conference on Disaster Prevention and Mitigation*, Montreal, QC, Canada, May.
- Huang, W.C., McClure, G. and Yao, G.C. (2010), "Shake table testing on moveable office partitions without top restraint", *Proceedings of the 9th US National and 10th Canadian Conference on Earthquake Engineering: Reaching Beyond Borders, EERI and CAEE*, Toronto, ON, Canada, July.
- ICC-ES (2010), *Acceptance criteria for seismic certification by shake-table testing of nonstructural components*, AC156, ICC-ES, Whittier, CA, USA.
- Jaimes, M.A., Reinoso, E. and Esteva, L. (2013), "Seismic vulnerability of building contents for a given occupancy due to multiple failure modes", *J. Earthq. Eng.*, **17**(5), 658-672.
- Lee, T., Kato, M., Matsumiya, T., Suita, K. and Nakashima, M. (2007), "Seismic performance evaluation of non-structural components: crywall partitions", *Earthq. Eng. Struct. D.*, **36**(3), 367-382.
- Loh, C.H. and Tsay, C.Y. (2001), "Responses of the earthquake engineering research community to the Chi-Chi (Taiwan) earthquake", *Earthq. Spectra*, **17**(4), 635-656.
- McMullin, K. and Merrick, D. (2007), "Seismic damage thresholds for Gypsum Wallboard partition walls", *J. Archit. Eng.*, **13**(1), 22-29.
- Retamales, R., Mosqueda, G., Filiatrault, A. and Reinhorn, A.M. (2011). "Testing protocol for experimental seismic qualification of distributed nonstructural systems", *Earthq. Spectra*, **27**(3), 835-856.
- Retamales, R., Davies, R., Mosqueda, G. and Filiatrault, A. (2013), "Experimental seismic fragility of cold-formed steel framed Gypsum partition walls", *J. Struct. Eng. - ASCE*, **139**(8), 1285-1293.
- Ryu, K.P., Reinhorn, A.M. and Filiatrault, A. (2012), "Full scale dynamic testing of large area suspended ceiling system", *Proceedings of 15th world conference on earthquake engineering (15WCEE)*, Lisbon, Portugal, September.
- Shin, T.C. and Teng, T.L. (2001), "An overview of the 1999 Chi-Chi, Taiwan", *Earthquake Bulletin of the Seismological Society of America*, **91**(5), 895-913.
- Yao, G.C. (2000), "Seismic performance of direct hung suspended ceiling systems", *J. Archit. Eng. - ASCE*, **6**(1), 6-11.